The Astrophysical Journal, 659:L111–L114, 2007 April 20

OCCULTATION MEASUREMENT OF THE SIZE OF THE X-RAY–EMITTING REGION IN THE ACTIVE GALACTIC NUCLEUS OF NGC 1365

G. Risaliti,[1,2] M. Elvis,[1] G. Fabbiano,[1] A. Baldi,[1] A. Zezas,[1] and M. Salvati[2]
Received 2007 February 14; accepted 2007 March 7; published 2007 March 16

ABSTRACT

We present an occultation of the central X-ray–emitting region in the Seyfert galaxy NGC 1365. This extreme spectral variation (from Compton-thin to reflection-dominated and back to Compton-thin in 4 days) has been caught in a 10 day *Chandra* monitoring campaign consisting of six short (15 ks) observations performed every 2 days. We discuss the implications of this occultation within the scenario of a Compton-thick cloud crossing the line of sight of the X-ray source. We estimate a source size $R \leq 10^{14}$ cm and a distance of the cloud from the source $D \leq 10^{16}$ cm. This direct measurement confirms the theoretical expectations of an extremely compact X-ray source and shows that the Compton-thick circumnuclear gas is located at a distance from the center on the scale of the broad-line region.

Subject headings: galaxies: active — galaxies: individual (NGC 1365)

Online material: color figures

1. INTRODUCTION

Variability of the X-ray–absorbing gas is common in active galactic nuclei (AGNs) on timescales from months to years (Risaliti et al. 2002). If an observed variation of absorbing column density N_H is due to clouds in virialized motion crossing the line of sight, the amount and the duration of the N_H variation put constraints on the distance of the obscuring cloud from the center and on the density of the cloud.

In a few cases, an N_H variation has been detected within a single observation (NGC 4388: Elvis et al. 2004; NGC 4151: Puccetti et al. 2007), indicating that the absorber must be extremely compact, i.e., on the scale of or slightly larger than the broad-line region ($\sim 10^{16}$ cm for a $10^8\ M_\odot$ black hole).

In this context, the Seyfert galaxy NGC 1365 has shown extreme variability in the past ~12 years: it was observed in a reflection-dominated state by *ASCA* in 1995 (Iyomoto et al. 1997), then in a Compton-thin state by *BeppoSAX* in 1997, with an absorbing column density $N_H \sim 4 \times 10^{23}$ cm^{-2} (Risaliti et al. 2000). Such a long time interval between the observations leaves two possible scenarios open: extreme absorption variability [$\Delta(N_H) > 10^{24}$ cm^{-2}] or a switch off and on of the X-ray source. This ambiguity has been solved with a more recent set of short observations, performed by *Chandra* in 2002 December 2002 and by *XMM-Newton* 3 and 6 weeks later. The source was caught in a reflection-dominated state in the first and third observations, while it was in a Compton-thin state with $N_H \sim 4 \times 10^{23}$ cm^{-2} in the second observation (Risaliti et al. 2005a, hereafter R05). Such fast variations are hard to explain within the intrinsic variation scenario, strongly suggesting that the observed reflection-dominated states are due to Compton-thick clouds crossing the line of sight (see R05 for a full discussion). Three additional *XMM-Newton* observations performed in 2003 and 2004 caught the source in a Compton-thin state, with column densities between 1.5 and 5×10^{23} cm^{-2}.

The latest two observations are relatively long (60 ks) and allowed for detailed timing and spectral analysis. The spectral analysis revealed the presence of a highly ionized, compact absorber (Risaliti et al. 2005b), while the timing analysis revealed column density variability of $\Delta(N_H) \sim 10^{23}$ cm^{-2} on timescales of ~50 ks (Risaliti 2007; G. Risaliti et al. 2007, in preparation).

In order to explore the variability timescales between the longest single observations (~1 day) and the shortest observed Compton-thick/Compton-thin change (3 weeks), we conducted a *Chandra* campaign consisting of six 15 ks observations performed once every ~2 days for 10 days in 2006 April. Here we report the results of these observations, with emphasis on an occultation event that occurred during the first 4 days of monitoring, and we discuss the physical implications of these results.

2. REDUCTION AND DATA ANALYSIS

The observation log is shown in Table 1. All the observations were performed with the ACIS-S instrument (Weisskopf et al. 2002) in "1/4 window" mode in order to avoid possible pileup. A check of the reduced spectra confirmed that in all cases, the pileup is lower than 1%.

The data were reduced using the CIAO 3.3 package and using a standard procedure, as described in the CIAO threads.[3] We extracted the spectrum from a circular region with a 2″ radius. This removes most of the soft, diffuse emission from the spectra (see Fig. 1 in R05). A complete analysis of the spectral and spatial properties of the diffuse component will be presented elsewhere (S. Bianchi et al. 2007, in preparation). The background was selected from a region in the field free from contaminating sources. The spectral analysis was performed using the Sherpa package inside CIAO.

A simple visual inspection of the spectra (Fig. 1) is enough to notice the main result of this work: the second spectrum is completely different from the others both in flux (it is much fainter) and in shape (it is flatter, with a prominent emission feature at ~6.5 keV), indicating that the source switched to a reflection-dominated state between the first and second observations, and then switched back to a transmission-dominated state between the second and the third observations.

We first performed a simple spectral analysis, with a model

[1] Harvard-Smithsonian Center for Astrophysics, Cambridge, MA 02138; grisaliti@cfa.harvard.edu.
[2] INAF–Osservatorio di Arcetri, Firenze 50125, Italy.

[3] See http://asc.harvard.edu/ciao/.

TABLE 1
NGC 1365: Observation Log of Six New *Chandra* ACIS-S Observations Started on 2006 April 14

OBS	Delay[a] (ks)	Duration (ks)	Rate (0.5–3 keV) (counts s^{-1})	Rate (3–10 keV) (counts s^{-1})
1	0	13.86	3.6×10^{-2}	6.1×10^{-2}
2	178	15.16	3.3×10^{-2}	2.2×10^{-2}
3	197	15.18	3.5×10^{-2}	5.6×10^{-2}
4	228	15.15	3.2×10^{-2}	10.2×10^{-2}
5	212	16.12	3.4×10^{-2}	10.5×10^{-2}
6	229	15.09	3.3×10^{-2}	15.9×10^{-2}

[a] Time elapsed from the end of the previous observation.

consisting of a thermal emission at low energies, an absorbed power law, and an iron emission line with $E = 6.4$ keV. In all the fits discussed below, the soft component is fitted with a thermal component (Raymond & Smith 1977) with temperature $kT = 0.8$ keV and constant within 2% in all cases.

All the high-energy ($E = 2$–10 keV) spectra, except for the second one, are well fitted (reduced χ^2 between 1.1 and 1.5) with a power law with photon index $\Gamma = 1.8$–2, a column density $N_H = (2$–$4) \times 10^{23}$ cm^{-2}, and an iron line with equivalent width EW = 200–300 eV. The second spectrum is fitted by a flat power law with $\Gamma \sim 0.5$ and $N_H < 10^{21}$ cm^{-2}. The emission feature has an equivalent width EW ~ 1.5 keV.

These results confirmed the visual inspection and prompted a more detailed analysis, which has been performed in two main steps: (1) We fitted the second spectrum with a cold reflection continuum (PEXRAV model; Magdziarz & Zdziarski 1995) and an emission line at 6.4 keV, corresponding to neutral iron Kα emission. A second line at energy $E = 6.9$ keV, corresponding to hydrogen-like iron, is also required by the fit. The photon index of the intrinsic component is not well constrained, so we fixed it to the average of the values obtained by fitting the transmission-dominated spectra. The best-fit equivalent widths of the two lines are $EW_{6.4} = 1.2 \pm 0.2$ keV and $EW_{6.9} = 0.9 \pm 0.4$ keV. (2) The other five spectra were fitted with the same reflection continuum (with all the parameters frozen to the best-fit values obtained in the analysis of the second spectrum) plus a continuum component representing the direct emission of the X-ray source. Since the spectra obtained in the past *XMM-Newton* observations have a much higher signal-to-noise ratio, we used the best-fit models obtained from those observations as a baseline for our spectral fitting. The best-fit model consists of an absorbed power law, plus four narrow absorption lines between 6.7 and 8.3 keV (representing He-like and H-like iron Fe Kα and Kβ transitions), and a broad emission line. We refer to Risaliti et al. (2005b) for a detailed description of these models.

The results of the fits are in all cases satisfactory from a statistical point of view (reduced χ^2 between 1 and 1.2) and provide best-fit values for the continuum photon index constant within the errors, while the values of the column density show significant variations. We then repeated the whole analysis by fitting all the spectra simultaneously, requesting a constant value for the photon index and leaving the other parameters free to vary. We obtained as good a fit as in the previous case from a statistical point of view (overall reduced $\chi^2 = 1.01$) and slightly smaller error intervals for the column density estimates. As a side product of our analysis, we mention that the two strongest iron absorption lines (Kα lines from He-like and H-like iron) are significantly detected. The inclusion of these features in the fit is relevant in our context only because neglecting them would affect the estimate of the continuum parameters. However, their detection is an interesting independent confirmation of the highly ionized absorber discovered in the *XMM-Newton* observations (Risaliti et al. 2005b). We will discuss this issue elsewhere (G. Risaliti et al. 2007, in preparation).

The main best-fit parameters are shown in Table 2.

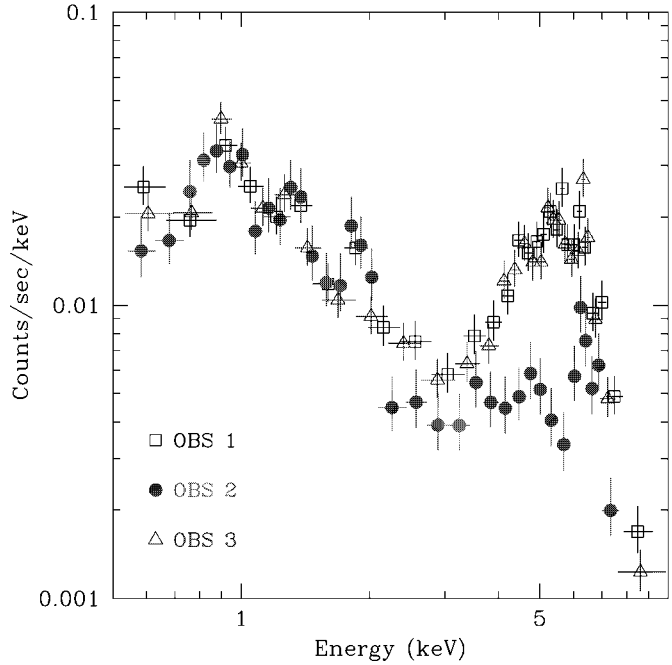

Fig. 1.—Spectra obtained from the first three *Chandra* observations of NGC 1365. The time interval between the single observations is 2 days. The first and third spectra are typical of a transmission-dominated source, with a steep continuum and a photoelectric cutoff at ~4 keV. The second spectrum is fainter by a factor ~10 and is characterized by a flat continuum and a prominent iron emission line, typical of reflection-dominated sources. The last three *Chandra* observations are similar to the first and third ones; for clarity, they are not shown. [*See the electronic edition of the Journal for a color version of this figure.*]

3. DISCUSSION

The analysis described in the previous section shows that a change from Compton-thin to Compton-thick states and then back to Compton-thin occurred in the first 4 days of our *Chandra* monitoring of NGC 1365.

As discussed in R05, such rapid changes are hard to explain with intrinsic spectral variations. In order to further check this

TABLE 2
NGC 1365: Spectral Fits

OBS	Γ	N_H[a]	$N_{H,2}$[b]	A[c]	R[d]
1	$1.4^{+1.1}_{-0.4}$	46^{+11}_{-12}	40^{+6}_{-3}	$3.7^{+0.8}_{-0.7}$	0.7 ± 0.2
2	1.7[e]	>100	>100	$2.6^{+0.8}_{-0.9}$	...
3	$2.7^{+1.5}_{-1.0}$	60^{+19}_{-13}	49^{+6}_{-6}	$3.1^{+0.7}_{-0.6}$	0.8 ± 0.2
4	$1.8^{+0.7}_{-0.6}$	36^{+7}_{-7}	34^{+3}_{-3}	$4.3^{+0.5}_{-0.5}$	0.6 ± 0.1
5	$2.0^{+0.5}_{-0.6}$	44^{+7}_{-7}	41^{+3}_{-3}	$5.6^{+0.7}_{-0.6}$	0.5 ± 0.2
6	$1.4^{+0.4}_{-0.2}$	22^{+3}_{-2}	23^{+1}_{-1}	$4.6^{+0.2}_{-0.3}$	0.6 ± 0.1

[a] Column density, in units of 10^{22} cm^{-2}, obtained by fitting a model with a free photon index power law.
[b] Column density, in units of 10^{22} cm^{-2}, with the photon index frozen to the average value, $\langle\Gamma\rangle = 1.68$.
[c] Normalization of the power law, in units of 10^{-3} photons s^{-1} cm^{-2} keV^{-1}. In OBS 2, this refers to the intrinsic emission producing the observed reflected spectrum.
[d] Ratio between the normalizations of the reflection and transmission components.
[e] Fixed value.

possibility, we estimated the upper limit of a possible direct component in the reflection-dominated spectrum. Assuming a spectral shape analogous to that obtained for the first and third observations (which are quite similar both in flux and in spectral parameters; Table 2), the 90% upper limit to the direct flux is only 5% of that of observations one and three. A decrease of the intrinsic flux by a factor of 20 and then an increase back to the initial flux, besides implying an unlikely "fine-tuning" in order to reproduce the observed symmetry between the fading and recovery phases, would require a cooling time of at least 3–4 weeks in the framework of a Shakura-Sunyaev (1973) disk (see R05 for details), completely incompatible with our observed varation times. For this reason, in the following we will only discuss the occultation scenario.

In the simplest scheme, shown in Figure 2, the size of the X-ray–emitting source D_S is given by the obscuring cloud velocity V_K times the ingress/egress time T_1. The linear size of the obscuring cloud is $D_C > D_S$, and the distance between the cloud and the source is R. Since our goal is to put an upper limit on the source size, it is particularly important to discuss the upper limits on the estimates of these two parameters.

Here we discuss several constraints on V_K, T_1, and D_S:

Statistical limits on T_1.—The occultation event is characterized by two times (Fig. 2): the ingress/egress time $T_1 = D_S/V_K$ and the time during which the source remains completely obscured, $T_2 = (D_C - D_S)/V_K$. Considering the X-ray observational history of NGC 1365, we note that the source has been observed four times in a completely reflection-dominated state, while it has never been observed during the ingress/egress phase in any published observation. In order to check this, we reanalyzed all the past observations looking for (1) fast drops in the light curves of the transmission-dominated spectra, indicative of a possible occultation event during the observation, and (2) possible direct continuum components in the reflection-dominated spectra. The first check easily ruled out the possibility that such occultations happened during any observation (this would imply a drop by a factor of at least 10 in the hard X- ray [$E > 4$ keV] light curve, which would be easily detected). In the second check, we added a direct continuum component to the model of the reflection-dominated spectra, consisting of an absorbed power law. We required that the photon index and the absorbing N_H varied within the lowest and highest values measured in all the transmission-dominated spectra. In the three most recent reflection-dominated spectra, this extra component is not required, and the upper limit to the flux of this component is as low as 10% of the faintest transmission-dominated spectrum. The result for the *ASCA* observation is inconclusive, because of the lower signal-to-noise ratio. Also, in this case, the extra component is not statistically required, but a significant contribution cannot be ruled out. Therefore, we do not include this observation in our analysis. In summary in three cases the source was found in a completely reflection-dominated state, and in no cases was it caught during an ingress/egress. During an eclipse, the source is in the partial occultation phase (state 1) for a total time $2T_1$ and is totally covered (state 2) for a time T_2. The fraction of time in the completely obscured state is $f = T_2/T_{tot}$, where $T_{tot} = (2T_1 + T_2) < 4.2$ days based on our observations. We require that the probability of finding the source three times in state 2 but never in state 1 is $P = f^3 > 10\%$. This implies $T_2 > 0.46T_{tot}$ and $T_1 < 0.27T_{tot} < 1$ day. Furthermore, we get $T_2 > 1.7T_1$, and $D_C > 2.7D_S$.

Physical limits on V_K.—A first limit on V_K comes from the measured width of the iron emission line in the reflection-dominated spectra. Here we assume that the reflecting Compton-thick gas is the same one that is responsible for the occultations. This is in agreement with the available statistics: since during the whole observational history of the source the occurrence of Compton-thick states is 4/14, it is expected that the obscuring clouds cover a significant fraction, $\sim\frac{1}{3}$, of the solid angle as seen from the source, and therefore they are also expected to contribute significantly to the observed reflection (a typical fitting value of the PEXRAV parameter R, normalized to 1 for a half-solid angle coverage of the reflector, is indeed ∼0.6–0.8, as shown in Table 2). The best available estimate of the iron line width, W_{Fe}, comes from the *XMM-Newton* observation of the reflection-dominated state of NGC 1365. We obtain $W_{Fe} < 150$ eV, corresponding to a velocity $V < 7000$ km s^{-1}. The line width measures only the average line-of-sight velocity, while during the occultation the cloud velocity vector lies in the plane of the sky. Assuming circular orbits, this implies that the actual transverse velocity during occultation can be as large as $(\pi/2)V = 12{,}000$ km s^{-1}. Finally, using $T_1 < 1$ day, we obtain $D_S < 10^{14}$ cm.

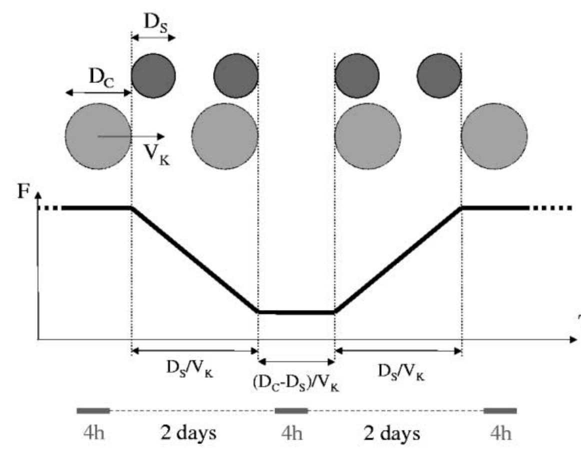

FIG. 2.—Schematic representation of the observed eclipse. The intervening thick cloud (*light gray circles*, diameter D_C) with Keplerian velocity V_K starts covering the X-ray source (*dark gray circles*, diameter D_S) at some time between the first and second *Chandra* observations. After a time $T_1 = D_S/V_K$, the source is completely covered and remains obscured for a time $T_2 = (D_C - D_S)/V_K$. In this state it is observed for the second time by *Chandra*. Then it gradually emerges until it is back in the initial state. After some more time, it is observed again by *Chandra*. From the times between the observations, we infer $T_2 + 2T_1 < 4$ days; $T_2 > 4$ hr. The lower part of the figure shows the time evolution of the observed flux. [*See the electronic edition of the Journal for a color version of this figure.*]

Geometrical limits on D_S.—A geometrical limit on D_S can be obtained by assuming the minimum possible distance R between the source and the cloud. This is given by $R = (D_S + D_C)/2$. Since the cloud size D_C must be equal to or larger than the source size D_S, the minimum distance for a given D_S is $R_{min} = D_S$. If the cloud is moving with Keplerian velocity $V_K = (GM_{BH}/D_S)^{1/2}$, the condition $V_K T_1 = D_S$ implies $D_S = (GM_{BH})^{1/3} T_1^{2/3}$.

Two independent estimates of the black hole mass in NGC 1365 are available: $\log(M_{BH}/M_\odot) = 7.3 \pm 0.4(0.3)$ from the M_{BH}–bulge velocity dispersion correlation (Oliva et al. 1995; Ferrarese et al. 2006) and $\log(M_{BH}/M_\odot) = 7.8 \pm 0.4(0.3)$ from the relation between M_{BH} and the K magnitude of the host bulge (Dong & De Robertis 2006; Marconi & Hunt 2003), where the errors include statistical and systematic effects, and the numbers in parentheses refer to the statistical dispersion of the correlation.

Using $T_1 < 1$ day, we obtain $D_S < 3 \times 10^{14}(M_{BH}/M_{est})^{1/3}$ cm, where M_{est} is the average estimate of the black hole mass according to the correlations cited above. Expressing the source size in units of gravitational radii, we find $D_S < 33(M_{BH}/M_{est})^{-2/3}R_G$. We note that the higher the black hole mass, the larger the physical size of the source, and the smaller the source size in units of gravitational radii. Considering the relatively high uncertainty in the black hole mass determination, we can repeat the above calculations using the minimum and maximum values compatible with the two correlations, $\log M_{BH(min)} = 7.1$ and $\log M_{BH(max)} = 8.0$. We obtain $D_S(\min) < 2 \times 10^{14}$ cm, corresponding to $56R_G$, and $D_S(\max) < 4.6 \times 10^{14}$ cm, corresponding to $15R_G$.

Physical limits on R.—A conceptually different limit on the distance R between the source and the obscuring cloud can be obtained by considering the ionization state of the latter. This is defined by the ionization parameter $U = L_X/(nR^2)$, where $n = N_H/D_C$ is the density of the obscuring cloud, located at a distance R from the central source, whose X-ray total luminosity is L_X. A limit on the ionization parameter can be obtained from the analysis of the reflection-dominated spectra observed with *XMM- Newton* and *Chandra*; we added to the best-fit model an extra component consisting of the continuum observed in transmission-dominated states, absorbed by gas with a variable column density and ionization parameter (Done et al. 1992). Since the upper limit on the flux of the direct emission is only a few percent of that observed in transmission-dominated states, the absorber must be effective enough to remove it almost completely. This implies a lower limit on the absorbing column density $N_H > 10^{24}$ cm^{-2} and an upper limit on the ionization parameter $U < U_{max} = 100$. From the latter limit, assuming that the cloud is moving with Keplerian velocity V_K and requiring that the cloud dimension D_C is larger than the source dimension D_S, we obtain, after a little algebra, $R > (GM_{BH})^{1/5}[(T_1 + T_2)L_X/(U_{max}N_H)]^{2/5}$. Assuming fiducial values for the occultation times and the cloud column density ($T_1 + T_2 \sim 2$ days and $N_H = 10^{24}$ cm^{-2}), we obtain $R > 3 \times 10^{15}(M_{BH}/M_{est})^{2/5}$ cm. We note that the dependence on the black hole mass is weak, so even adopting the extreme values allowed for M_{BH} would change the result by a factor of less than 30%. From this estimate we can easily obtain a new limit on the Keplerian velocity $V_K = (GM_{BH}/R)^{1/2} < 12{,}000(M_{BH}/M_{est})^{2/5}$ km s^{-1}, i.e., the same upper limit as used in the previous argument on the line width. Analogously, the limit on the source size is $D_S = V_K T_1 < 10^{14}(M_{BH}/M_{est})^{2/5}$ cm.

Summarizing the constraints on the source size, we obtained the following:

1. $D_S < 3 \times 10^{14}(M_{BH}/M_{est})^{1/3}$ cm (from geometrical considerations).
2. $D_S < 10^{14}$ cm (from the observed limits on V_K).
3. $D_S < 10^{14}(M_{BH}/M_{est})^{2/5}$ cm (from limits on the ionization state of the obscuring cloud).

All these independent methods strongly suggest that the X-ray source has a size of the order of or smaller than 10^{14} cm, corresponding to $10R_G$ for a black hole mass $M_{BH} = M_{est} = 3 \times 10^7\ M_\odot$.

We note that our estimates can be slightly altered if the case of a partial covering of the thick cloud in the first and third observations is considered. Specifically, in order to reproduce the observed symmetry in the first three observations, the same fraction F of the source should be covered in observations one and three. However, if the fraction F is small, the effect is negligible, while if F is big, the cloud would uncover the source in the subsequent observations, implying a large increase of the flux from the third to the fourth observation, which is not observed (Table 2). We conclude that the possible effect of the partial covering of the transmission-dominated spectra would not significantly affect our estimates of the source and cloud sizes.

Using the calculations discussed above, we can easily estimate the distance of the obscuring cloud from the center. Assuming $V_K = 12{,}000$ km s^{-1} and $M_{est} = 3 \times 10^7\ M_\odot$, we obtain $R = 3 \times 10^{15}$ cm, compatible with the lower limit deduced from the ionization condition. Such a distance corresponds to $300R_G$ and is of the same order of the distance from the center of the innermost broad-line clouds, and therefore much more compact than the circumnuclear medium assumed in the standard unified models of AGNs (e.g., Krolik & Begelman 1988).

This work has been partially funded by NASA grant G06-7102X. We also acknowledge the financial contribution from contract ASI-INAF I/023/05/0.

REFERENCES

Done, C., Mulchaey, J. S., Mushotzky, R. F., & Arnaud, K. A. 1992, ApJ, 395, 275
Dong, X. Y., & De Robertis, M. M. 2006, AJ, 131, 1236
Elvis, M., Risaliti, G., Nicastro, F., Miller, J. M., Fiore, F., & Puccetti, S. 2004, ApJ, 615, L25
Ferrarese, L., et al. 2006, ApJ, 644, L21
Iyomoto, N., Makishima, K., Fukazawa, Y., Tashiro, M., & Ishisaki, Y. 1997, PASJ, 49, 425
Krolik, J. H., & Begelman, M. C. 1988, ApJ, 329, 702
Magdziarz, P., & Zdziarski, A. A. 1995, MNRAS, 273, 837
Marconi, A., & Hunt, L. K. 2003, ApJ, 589, L21
Oliva, E., Origlia, L., Kotilainen, J. K., & Moorwood, A. F. M. 1995, A&A, 301, 55
Puccetti, S., Fiore, F., Risaliti, G., Capalbi, M., Elvis, M., & Nicastro, F. 2007, MNRAS, in press (astro-ph/0612021)
Raymond, J. C., & Smith, B. W. 1977, ApJS, 35, 419
Risaliti, G. 2007, preprint (astro-ph/0701108)
Risaliti, G., Bianchi, S., Matt, G., Baldi, A., Elvis, M., Fabbiano, G., & Zezas, A. 2005a, ApJ, 630, L129 (R05)
Risaliti, G., Elvis, M., Fabbiano, G., Baldi, A., & Zezas, A. 2005b, ApJ, 623, L93
Risaliti, G., Elvis, M., & Nicastro, F. 2002, ApJ, 571, 234
Risaliti, G., Maiolino, R., & Bassani, L. 2000, A&A, 356, 33
Shakura, N. I., & Sunyaev, R. A. 1973, A&A, 24, 337
Weisskopf, M. C., Brinkman, B., Canizares, C., Garmire, G., Murray, S., & Van Speybroeck, L. P. 2002, PASP, 114, 1